Jackson, V. (1978) *Cell (Cambridge, Mass.) 15*, 945-954.
Jackson, V. (1987a) *Biochemistry 26*, 2315-2324.
Jackson, V. (1987b) *Biochemistry 26*, 2325-2333.
Jackson, V., & Chalkley, R. (1981a) *Cell (Cambridge, Mass.) 23*, 121-134.
Jackson, V., & Chalkley, R. (1981b) *J. Biol. Chem. 256*, 5095-5103.
Jackson, V., & Chalkley, R. (1985a) *Biochemistry 24*, 6921-6930.
Jackson, V., & Chalkley, R. (1985b) *Biochemistry 24*, 6930-6938.
Jackson, V., Granner, D. K., & Chalkley, R. (1975) *Proc. Natl. Acad. Sci. U.S.A. 72*, 4440-4444.
Jackson, V., Marshall, S., & Chalkley, R. (1981) *Nucleic Acids Res. 9*, 4563-4580.
Laemmli, U. K. (1970) *Nature (London) 227*, 680-683.
Laskey, R. A., & Mills, A. D. (1979) *Eur. J. Biochem. 56*, 335-342.
Leffak, I. M. (1983) *Nucleic Acids Res. 11*, 2712-2732.
Leffak, I. M. (1984) *Nature (London) 307*, 82-85.
Leffak, I. M., Grainger, R., & Weintraub, H. (1977) *Cell (Cambridge, Mass.) 12*, 837-846.
Louters, L., & Chalkley, R. (1984) *Biochemistry 23*, 547-552.
Manser, T., Thacher, T., & Rechsteiner, M. (1980) *Cell (Cambridge, Mass.) 19*, 993-1003.
McGhee, J. D., & Felsenfeld, G. (1980) *Annu. Rev. Biochem. 49*, 1115-1156.
McGhee, J. D., & Felsenfeld, G. (1983) *Cell (Cambridge, Mass.) 32*, 1205-1215.
Pospelov, V., Russev, G., Vassilov, L., & Tsanev, R. (1982) *J. Mol. Biol. 156*, 79-91.
Prior, C. P., Cantor, C. R., Johnson, E. M., & Allfrey, V. G. (1980) *Cell (Cambridge, Mass.) 20*, 597-608.
Prior, C. P., Cantor, C. R., Johnson, E. M., Littau, V. C., & Allfrey, V. G. (1984) *Cell (Cambridge, Mass.) 34*, 1033-1042.
Russev, G., & Hancock, R. (1982) *Proc. Natl. Acad. Sci. U.S.A. 79*, 3143-3147.
Ryoji, M., & Worcel, A. (1984) *Cell (Cambridge, Mass.) 37*, 21-32.
Saragosti, S., Cereghini, S., & Yaniv, M. (1982) *J. Mol. Biol. 160*, 133-146.
Seidman, M. M., Levine, A. J., & Weintraub, H. (1979) *Cell (Cambridge, Mass.) 18*, 439-449.
Senshu, T., Fukuda, M., & Ohashi, M. (1978) *J. Biochem. (Tokyo) 84*, 985-988.
Senshu, T., Yamasu, K., & Ohsawa, T. (1985) *Eur. J. Biochem. 150*, 575-580.
Simon, R. H., Camerini-Otero, R. D., & Felsenfeld, G. (1978) *Nucleic Acids Res. 5*, 4805-4818.
Sogo, J. M., Stahl, H., Koller, T., & Knippers, R. (1986) *J. Mol. Biol. 189*, 189-204.
Stein, A., Bina-Stein, M., & Simpson, R. T. (1977) *Proc. Natl. Acad. Sci. U.S.A. 74*, 2780-2784.
Stein, A., Holley, K., Zeliff, J., & Townsend, T. (1985) *Biochemistry 24*, 1783-1790.
Varshavsky, A. J., Sundin, O., & Bohn, M. (1979) *Cell (Cambridge, Mass.) 16*, 453-466.
Villeponteau, B., Lundell, M., & Martinson, H. (1984) *Cell (Cambridge, Mass.) 39*, 469-478.
Waithe, W. I., Renaud, J., Nadeau, P., & Pallotta, D. (1983) *Biochemistry 22*, 1778-1783.
Wray, W., Boulikas, T., Wray, V. P., & Hancock, R. (1981) *Anal. Biochem. 118*, 197-203.
Wu, R. S., & Bonner, W. M. (1981) *Cell (Cambridge, Mass.) 27*, 321-330.
Wu, R. S., Kohn, K. W., & Bonner, W. M. (1981) *J. Biol. Chem. 256*, 5916-5920.
Wu, R. S., Tsai, S., & Bonner, W. M. (1982) *Cell (Cambridge, Mass.) 31*, 367-374.
Yamasu, K., & Senshu, T. (1987) *J. Biochem. (Tokyo) 101*, 1041-1049.

Optical Properties of Tb^{3+}-Phospholipid Complexes and Their Relation to Structure†

Helen N. Halladay and Matthew Petersheim*
Department of Chemistry, Seton Hall University, South Orange, New Jersey 07079
Received September 9, 1987; Revised Manuscript Received November 19, 1987

ABSTRACT: The excitation and emission properties of Tb^{3+}-phospholipid complexes are shown to provide structural and dynamic information about the general ligand field of the bound lanthanide. Most of the conclusions derive from the relative behavior of 4f to 5d and 4f to 4f electronic transitions of Tb^{3+}. These observations demonstrate the unique properties of Tb^{3+} as a probe of cation binding sites on phospholipid membranes and its potential in describing changes in the lipid phase state.

Among the several parameters which can alter the phase behavior of phospholipid membranes, cation binding can induce some of the most dramatic, e.g., lateral phase separation (Graham et al., 1985; Wilschut et al., 1985; Leventis et al., 1986), intramembrane inverted micelle formation (Bearer et al., 1982; Verkleij, 1984; Smaal et al., 1987a,b), and membrane fusion (Sundler & Papahadjopoulos, 1981; Sundler et al., 1981; Bearer et al., 1982; Duzgunes et al., 1984; Wilschut et al., 1985; Leventis et al., 1986). The objective of a wide range of studies involving nuclear magnetic resonance (Hauser et al., 1975; Grasdalen et al., 1977; Baruskov et al., 1980; Chrzeszczyk et al., 1981; McLaughlin, 1982; Altenbach & Seelig, 1984; Miner & Prestegard, 1984), infrared (Dluhy et

† This research was supported by a Cottrell Grant from the Research Corp.

0006-2960/88/0427-2120$01.50/0

al., 1983; Conti et al., 1987), electron spin resonance (Boggs & Rangaraj, 1983), ultrasonic absorption (Aruga et al., 1985), and X-ray diffraction (McIntosch, 1980; Caffrey & Feigenson, 1984) is to establish the structural basis for these induced phase changes. Here, and in previous studies (Saris, 1983; Hermann et al., 1986; Conti et al., 1987), the optical properties of the luminescent trivalent lanthanides have been shown to provide useful information about the structure of cation binding sites on phospholipid membranes. The emphasis of this work is on the excitation spectrum of several Tb^{3+}–phospholipid complexes. These results demonstrate the potential of Tb^{3+} as a probe of cation-induced phase changes and of site competition among membrane-bound cations. The optical properties of Tb^{3+} and the other lanthanides are uniquely suited for the study of transient cation–phospholipid states such as those expected during membrane fusion.

Materials and Methods

Dihexanoylphosphatidylcholine (DHPC),[1] DLPC, DMPC, DMPG, DMPS, DMPE, DMPA, DOPA, DOPC, DPPC, DPrPC, lyso-MPC, and beef heart cardiolipin were purchased from Avanti Polar Lipids, Inc. (Birmingham, AL), and used as received. $TbCl_3$ and NaCl were dried to a constant weight in a vacuum oven and concentrations of stock solutions determined by weight of the solute. All lipid solutions were prepared with 100 mM NaCl except cardiolipin which was prepared with distilled water. All concentrations were determined by weight. The final pH of the lipid solutions was found to be, or adjusted to be, between 6.0 and 7.0, except DMPE which was left between 7.0 and 7.5. Addition of $TbCl_3$ had no measurable effect on pH. The stock lipid solutions were sonicated until mixed, and then 1.0-mL aliquots were pipetted into small glass vials along with an appropriate amount of $TbCl_3$ (50 μL or less of a concentrated stock solution). Each sample was further sonicated until no change in clarity was observed (15–60 min) using a 300-Watt sonic dismembrator (Fisher) with a 25-mL jacketted bath attachment. The temperature in the sonicator bath was maintained above the phase transition temperature for each lipid. All cardiolipin samples were kept under a positive pressure of nitrogen to minimize oxidation of the unsaturated fatty acid chains. Tb^{3+} binding to the phospholipid vesicles was measured by equilibrium dialysis, as discussed previously (Conti et al., 1987).

All spectra were collected on a spectrofluorometer equipped with double-quartermeter monochromators and photon counting detection. Excitation spectra were collected with a 150-W Xe flash lamp operating at 20 Hz, using a band-pass of 5.4 nm on the excitation monochromator and a 14.4-nm band-pass for the emission monitored at 545 nm. The flash lamp was used to minimize wavelength-dependent background due to light scattering by the lipid vesicles. No correction was made for lamp profile and instrument throughput, but a background spectrum of the lipid with no Tb^{3+} was subtracted from all excitation spectra. No evidence of fluorescent or phosphorescent impurities in the phospholipid suspensions was detected. Emission spectra (supplementary material; see paragraph at end of paper regarding supplementary material) were collected with a 450-W continuous Xe lamp using a 1.2-nm band-pass on the emission monochromator and were corrected for the throughput of the instrument. The excitation wavelength depended on the particular Tb^{3+}–phospholipid complex. Low-pass and high-pass filters were used in the excitation and emission pathways in order to minimize scattering effects. Quartz cells having a 4-mm excitation path length were used to alleviate the inner filter effect due to light scattering by the sample. Cell temperature was maintained at 30 °C by a jacketted turret and a circulating bath.

[1] Abbreviations: DHPC, dihexanoylphosphatidylcholine; DLPC, dilauroylphosphatidylcholine; DMPA, dimyristoylphosphatidic acid, monoprotic; DMPC, dimyristoylphosphatidylcholine; DMPG, dimyristoylphosphatidylglycerol; DMPS, dimyristoylphosphatidylserine; DOPA, dioleoylphosphatidic acid; DOPC, dioleoylphosphatidylcholine; DPPC, dipalmitoylphosphatidylcholine; DPrPC, dipropionoylphosphatidylcholine; lyso-MPC, monomyristoyllysophosphatidylcholine.

Table I: Excitation Properties of Tb^{3+}–DMPC Complexes

excitation wavelength (nm)	relative molar emission[a]		
	aquo-Tb^{3+}	DMPC(I)[b]	DMPC(II)[c]
250	0.16	16	1.4
261	1.00	31	3.8
285	0.44	219	5.8
298	0.08	349	5.7
307	0.06	212	3.9
351	0.47	5	1.1

[a] Intensity of the emission at 545 nm (14.4-nm band-pass) divided by the molar concentration of the Tb^{3+} species indicated. All values are normalized to the 261-nm excitation band of aquo-Tb^{3+}. [b] Estimated from the spectrum of 0.029 mM Tb^{3+} and 2 mM DMPC by using the parameters from Conti et al. (1987) to determine total bound Tb^{3+} and the amount in each bound state. [c] Estimated from the spectrum of 0.36 mM Tb^{3+} and 2 mM DMPC by using the parameters from Conti et al. (1987) to determine total bound Tb^{3+} and the amount in each bound state.

Results

Aquo-Tb^{3+} has several forbidden 4f to 4f absorption bands in the ultraviolet region with extinction coefficients less than 0.4 M^{-1} cm^{-1}, a forbidden 4f to 5d band at 263 nm with a coefficient of 1 M^{-1} cm^{-1}, and an allowed 4f to 5d band at 217 nm with a coefficient of 300 M^{-1} cm^{-1} (Carnall et al., 1968). Excitation by way of any of these bands yields emission with the same quantum yield (Horrocks & Albin, 1984). There are four well-resolved emission bands between 450 and 650 nm that arise from a common 4f $^5D_4$ excited state and different 4f ^7F_J ground states (Hufner, 1978; Horrocks & Albin, 1984). Of these four bands, the $^5D_4$ to $^7F_5$ transition centered at 545 nm is the most intense and was monitored for all excitation and emission studies. In dilute aqueous solution Tb^{3+} exists as the 9-coordinate aquo species (Horrocks & Albin, 1984). Up to eight of the water molecules are displaced upon binding to phospholipids, most likely by the phosphate groups of the lipids (Herrmann et al., 1986). Displacement of water from the inner coordination sphere of Tb^{3+} removes an important source of nonradiative decay; hence, an increase in lifetime and quantum yield is observed.

Tb^{3+} Binding to Zwitterionic Lipids. In a previous study of Tb^{3+} binding to DMPC (Conti et al., 1987), the intensity of the 545-nm emission band was found to increase by much more than could be due to displacement of quenching water molecules, and there was evidence of two Tb^{3+}-bound states related by an ionotropic phase transition. The extreme change observed in Tb^{3+} emission can now be attributed to a change in the extinction coefficient of the bound lanthanide. The excitation spectra for the two Tb^{3+}–DMPC complexes are shown in Figure 1a using low (solid line) and high (dashed line) Tb^{3+} concentrations to adjust the phase state. Excessive light scattering by the lipid vesicles prohibited excitation much below 240 nm. Figure 1b is the excitation spectrum of a 3.9 mM $TbCl_3$ solution, which is drastically different in appearance and relative intensity from that of either Tb^{3+}–DMPC complex. The forbidden 4f to 5d band which should be at 263 nm (Carnall et al., 1968) occurs at 261 nm here because the

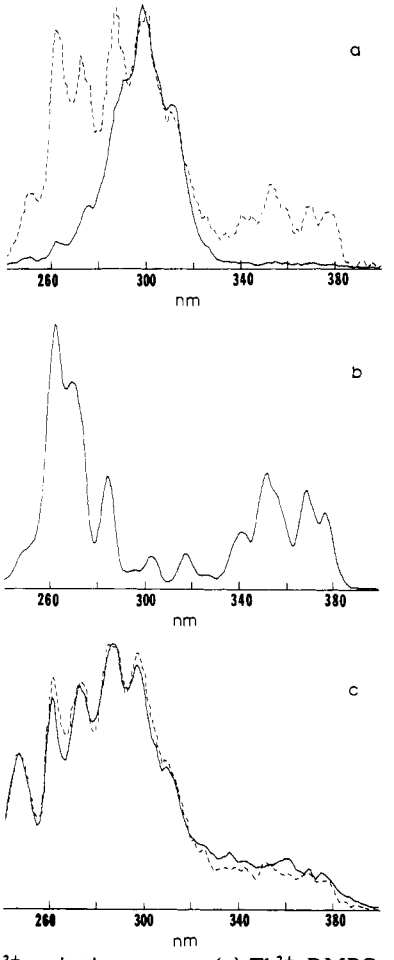

FIGURE 1: Tb^{3+} excitation spectra. (a) Tb^{3+}–DMPC complex with 0.035 mM $TbCl_3$ (solid line) and 0.40 mM $TbCl_3$ (dashed line) in 2 mM DMPC and 100 mM NaCl. (b) 3.9 mM aquo-Tb^{3+}. (c) Tb^{3+}–DMPE with 0.085 mM $TbCl_3$ (solid line) and 0.565 mM $TbCl_3$ (dashed line) in 2 mM DMPE and 100 mM NaCl.

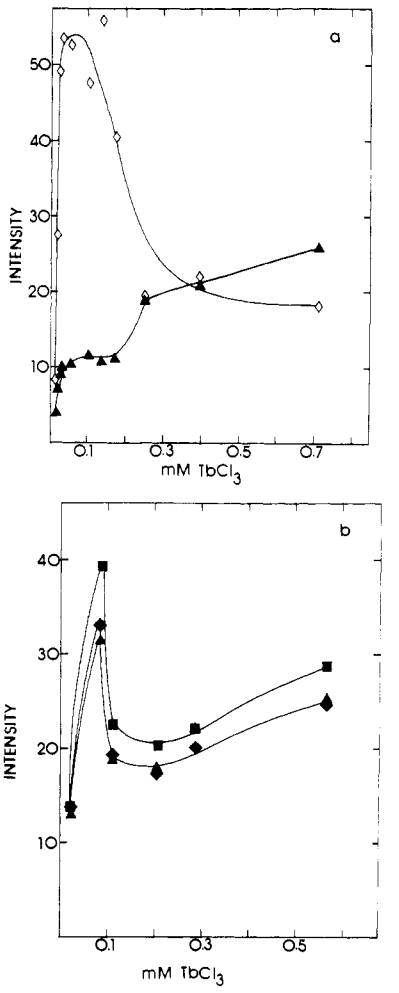

FIGURE 2: Concentration dependence of the Tb^{3+}–DMPC and Tb^{3+}–DMPE excitation bands. (a) Tb^{3+}–DMPC emission intensity with excitation at 261 nm (closed triangles) and 298 nm (open diamonds). Each point represents a separate DMPC sample (2 mM lipid and 100 mM NaCl) sonicated for 45–60 min above 30 °C. (b) Tb^{3+}–DMPE emission intensity using excitation bands at 261 nm (closed triangles), 271 nm (closed diamonds), and 286 nm (closed squares). Each point represents a separately prepared sample with 2 mM DMPE and 100 mM NaCl.

spectra were not corrected for the Xe lamp profile. Relative emission efficiencies for aquo-Tb^{3+} and the two Tb^{3+}–DMPC complexes at several excitation wavelengths are given in Table I. Plots of emission intensity vs Tb^{3+} concentration for the bands at 261 and 298 nm are given in Figure 2a to more clearly show the induced phase transition. Thermodynamic aspects of the transition are discussed in detail in Conti et al. (1987).

Both bound states have been observed with several other bilayer-forming phosphatidylcholines, namely, DPPC, DLPC, and DOPC, as well as two micelle-forming species, DHPC and lyso-MPC. Because of the lower turbidity of the lyso-MPC micelle solutions, it was possible to extend the excitation experiments to the allowed 4f to 5d band at lower wavelengths. These preliminary studies give strong evidence that the large band at 298 nm for Tb^{3+}–DMPC(I) derives from the allowed 4f to 5d transition. The magnitude of the band alone supports this assumption in that it obscures all other features in the spectrum (Figure 1a). This very large red shift, from 217 to 298 nm, for the allowed absorption band is indicative of an unusual coordination state in Tb^{3+}–DMPC(I). For Tb^{3+}–DMPC(II), the excitation properties are consistent with forbidden transitions and a return to what may be a more usual coordination state for the lanthanide.

The fact that lyso-MPC exhibits the same type of ionotropic transition as the bilayer-forming species argues against it being a simple matter of lipid packing distortion as a result of Tb^{3+} coordination. The transition is more likely a consequence of the deposited surface charge as was demonostrated in Ca^{2+}–phosphatidylcholine studies by Macdonald and Seelig (1987). In their deuterium NMR experiments, the quadrupole splitting of resonances from the choline head group was found to increase with the surface charge density under various conditions. X-ray diffraction studies of a La^{3+}–phosphatidylcholine complex demonstrated that the choline head group is forced out of the membrane plane as a result of complexation (McIntosch, 1980). The NMR experiments (MacDonald & Seelig, 1987) would suggest that this is a consequence of Coulombic repulsion between the quaternary amine of choline and the positive surface charge from bound cation. Changes in the Tb^{3+} excitation spectrum resulting from this transition (Figures 1a and 2a) are likely due to different conformations of the phosphate groups forced by repulsion of the choline chain. ^{13}C and ^{31}P NMR experiments intended to establish the structures of the two complexes are in progress.

DPrPC, a species which does not readily form bilayers or micelles, appears to have very low affinity for Tb^{3+} even under conditions which strongly favor binding to DMPC (Conti et al., 1987), such as 20 mM DPrPC, 0.3 mM Tb^{3+}, and 100 mM $NaClO_4$. The Tb^{3+} optical properties are identical with those of the aquo complex in this case. Thus, the high affinity of trivalent lanthanides for phosphatidylcholine membranes

Table II: Excitation Properties of Tb^{3+}–Anionic Lipid Complexes

excitation wavelength (nm)	relative molar emission[a] aquo-Tb^{3+}	DMPG	DMPS	DMPA I	DMPA II	cardiolipin I	cardiolipin II
245	0.05		6.3				
250	0.16	21		6.1	5.9	24	14
261	1.00	14	8.9	19	18	39	38
269	0.79		5.3	24	10		
285	0.44			10	7.0		
353	0.47	3.1	3.1	8.2	3.3		

[a] Confer Table I.

(Grasdalen et al., 1977; Chrzeszczyk et al., 1981; Conti et al., 1987) results from the high surface concentration of phosphate moieties and not an intrinsically strong interaction between the cation and phosphodiesters. This was demonstrated in earlier studies with dimethyl phosphate (Chrzeszczyk et al., 1981).

DMPE complexation of Tb^{3+} also exhibits a bimodal titration curve (Figure 2a) with excitation efficiencies roughly equal to those of the DMPC complexes and with the transition occurring at essentially the same level of Tb^{3+}, i.e., 20:1 lipid:Tb^{3+} ratio. Equilibrium dialysis experiments indicate that the lanthanide has approximately the same affinity for both zwitterionic lipids (unpublished results). The behavior of the Tb^{3+}–DMPE complexes deviates from those of DMPC in that the cation-induced transition is not accompanied by a change in appearance of the excitation spectrum (Figure 1c). In fact, the Tb^{3+}–DMPE excitation spectrum strongly resembles that of Tb^{3+}–DMPC(II) throughout the DMPE phase transition. These observations suggest that at high levels of bound Tb^{3+} its coordination is similar in DMPE and DMPC membranes, probably with the cationic head group of both lipids repelled from the surface. At low levels of bound Tb^{3+}, the coordination by the two lipids differs, probably as a result of constraints imposed by the glycerol tilt in phosphatidylcholine membranes. This tilt is removed at high levels of bound lanthanide (McIntosch, 1980) and does not exist with phosphatidylethanolamine or any of the other phospholipids. In corroboration of this statement, none of the other Tb^{3+}–phospholipid complexes exhibits the drastic red shift of the allowed 4f to 5d band observed with Tb^{3+}–DMPC(I) (vide infra). Since the bimodal behavior of the Tb^{3+}–DMPE excitation bands does not seem to reflect a change in coordination for the bound state, it is likely that the Tb^{3+}–DMPE phase transition leads to more rapid exchange between bound and aquo species. The bound state with its greater absorptivity would dominate the excitation spectrum, but the overall quantum yield would be diminished by exchange to the more severely quenched aquo species. This explanation is consistent with a more exposed binding site, i.e., displacement of head groups from the membrane surface; however, careful relaxation studies would be required to establish this point.

Tb^{3+} Binding to Anionic Lipids. Complexes of Tb^{3+} with four different anionic phospholipids, DMPA, DMPS, DMPG, and bovine heart cardiolipin, each yield a unique excitation spectrum (Figure 3). Only two of these, DMPA and cardiolipin, give evidence of more than one Tb^{3+}-bound state. Figure 4 shows the intensities of a few excitation bands versus Tb^{3+} concentration for both of these lipids. Titrations of DMPS and DMPG yield linear increases in emission intensity up to the point of precipitation, with no variation in the appearance of the Tb^{3+} excitation spectrum. Equilibrium dialysis demonstrates that virtually all of the Tb^{3+} is bound to the

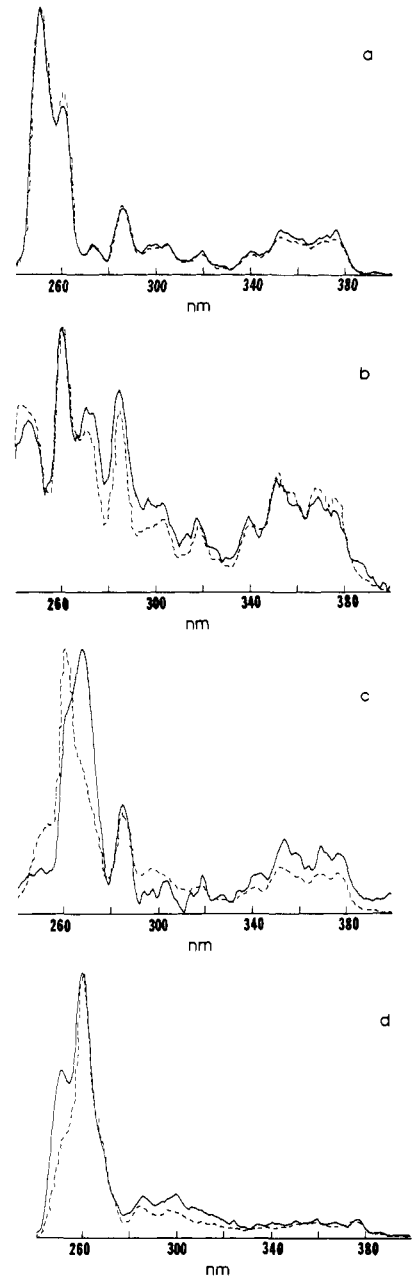

FIGURE 3: Excitation spectra of the Tb^{3+}–anionic lipid complexes at low (<0.05 mM, solid line) and high (>0.250 mM, dashed line) $TbCl_3$ concentrations. (a) Tb^{3+}–DMPG; (b) Tb^{3+}–DMPS; (c) Tb^{3+}–DMPA; (d) Tb^{3+}–cardiolipin. All lipid concentrations are 2 mM lipid except cardiolipin which is 1 mM lipid.

anionic lipids up to stoichiometric levels of the cation (unpublished data). The relative emission efficiencies for all four anionic lipids are given in Table II.

The titration curves for DMPA (Figure 4a) reflect competition between two Tb^{3+}-bound states. The nature of these states is suggested by a similar set of experiments performed with DOPA. The appearance of the Tb^{3+}–DOPA excitation spectrum is invariant with the level of bound Tb^{3+} and is identical with that of the second DMPA state, Tb^{3+}–DMPA-(II). The intensity of the Tb^{3+}–DOPA excitation bands increases linearly with Tb^{3+} concentration, as with Tb^{3+}–DMPS and Tb^{3+}–DMPG. The principal difference between these two phosphatidic acids is the greater surface area per DOPA resulting from poorer packing of the unsaturated oleoyl chains. At present, it seems most likely that the two Tb^{3+}–DMPA states are $Tb^{3+}\cdot(DMPA^{1-})_3$ and $Tb^{3+}\cdot(DMPA^{1-})_2$; in Tb^{3+}–DOPA, the tris-$DOPA^{1-}$ complex is prohibited by acyl chain

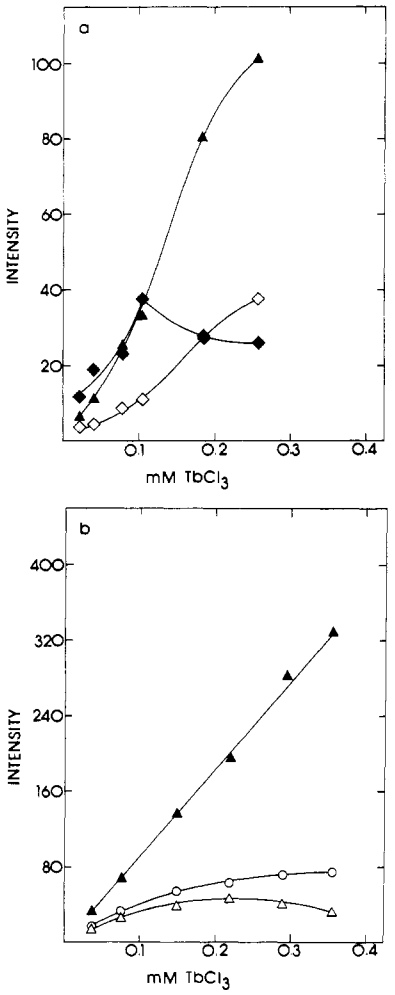

FIGURE 4: Concentration dependence of the Tb^{3+}–DMPA and Tb^{3+}–cardiolipin excitation bands. (a) Tb^{3+}–DMPA emission intensity using excitation at 251 nm (open diamonds), 261 nm (closed triangles), and 270 nm (closed diamonds). (b) Tb^{3+}–cardiolipin emission intensity using excitation at 248 nm (open circles), 252 nm (open triangles), and 261 nm (closed triangles). The intensities of the overlapping Tb^{3+}–DMPA bands at 261 and 269 nm and Tb^{3+}–cardiolipin bands at 252 and 261 nm were obtained by assuming Lorentzian band shapes with a 10-nm width.

packing, leaving only $Tb^{3+}\cdot(DOPA^{1-})_2$. Several attempts were made to confirm these stoichiometries by ^{31}P NMR using various paramagnetic lanthanides; however, the results were complicated by slow chemical exchange of the bound lanthanide and precipitation. A more rigorous set of optical experiments are in progress which will permit quantitative interpretation of the equilibrium reflected in Figure 4a.

Titration of cardiolipin with Tb^{3+} yields an excitation spectrum varying with bound lanthanide in a manner subtlely different from Tb^{3+}–DMPC, Tb^{3+}–DMPE, and Tb^{3+}–DMPA. The strong band at 261 nm increases linearly in intensity with bound Tb^{3+} whereas all other bands approach asymptotic levels (Figures 3d and 4b). The simplest explanation for this observation is that the 261-nm band of Tb^{3+}–cardiolipin is the forbidden 4f to 5d band. Its position and molar emission do not vary with the level of bound Tb^{3+} (Table II) because a single coordination state persists, and the other bands in the spectrum decrease in molar emission with increased Tb^{3+} because of changes in the lattice vibrations. In this last statement it is assumed that all of the absorption bands shown in Figure 3d result from 4f to 4f transitions, except the 261-nm band. Since all of the absorption bands of Tb^{3+} have the same emission quantum yields (Horrocks & Albin, 1984), the differential behavior between the 4f to 5d transition and the 4f to 4f transitions probably arises from the latter being more dependent on vibrational mixing of allowed character to the transition dipole (Hufner, 1978; Blasse, 1979; Jorgensen, 1979; Carnall, 1979; Reid & Richardson, 1984). If it is assumed that the change in the Tb^{3+}–cardiolipin lattice reflected in 4f to 4f transitions is a consequence of a lamellar to hexagonal phase transition for the lipid (Verkleij, 1984), then these results indicate that Tb^{3+} coordination is unaffected by this change in phase state.

The shape and position of the 545-nm emission band for bound Tb^{3+} are also sensitive to the identity of the lipid head group, but not as dramatically as the excitation spectrum. Both the $^5D_4$ excited state and the $^7F_5$ ground state involved in this transition are multiply degenerate and can be split by the ligand field (Hufner, 1978). Comparison of the emission band shapes suggests that Tb^{3+}–DMPC(II) and Tb^{3+}–DMPE present similar ligand fields, Tb^{3+}–DMPS and Tb^{3+}–DMPG are similar, and Tb^{3+}–DMPA and Tb^{3+}–cardiolipin are very similar. These emission spectra are are available as supplementary material (see paragraph at end of paper regarding supplementary material).

Mixed Lipid Systems. Preliminary studies of Tb^{3+} binding to mixed lipid systems have given evidence for mixed lipid complexes and Ca^{2+}-induced changes in the coordination of bound Tb^{3+}. DMPA/DMPC and DOPA/DOPC mixtures, ranging from 1/1 to 1/20 mole ratios, yield Tb^{3+} excitation spectra which are linear combinations of Tb^{3+}–DMPA(II), Tb^{3+}–DMPC(I), and Tb^{3+}–DMPC(II) spectra, except for the relative intensity of a band at 250 nm. It is this last band which is presumed to be evidence for a mixed lipid complex. Again, ^{31}P NMR experiments intended to test this statement were complicated by slow exchange of the bound lanthanide.

Studies of Tb^{3+} binding to DMPS–DMPC and cardiolipin–phosphatidylcholine mixtures were performed before the excitation experiments were developed. In both cases, emission from low levels of bound Tb^{3+}, e.g., 1 Tb^{3+}/50 lipid molecules, could be used to monitor slow phase changes induced by the addition of Ca^{2+}. The time scale for the phase changes is on the order of second to hours, depending on the ionic strength and the levels of Tb^{3+} and Ca^{2+}. At present, there is no additional evidence for the nature of these phase changes, although it seems likely that with the DMPS–DMPC system it is a form of lateral phase separation (Wilschut et al., 1985) and with cardiolipin–phosphatidylcholine it may be inverted micelle formation (Verkleij, 1984).

Discussion

The results presented here demonstrate the sensitivity of the Tb^{3+} excitation spectrum to the identity of the phospholipid head groups to which it is bound, the phase state of the lipid, insofar as it alters head-group packing, and, possibly, changes in lattice dynamics as they affect the vibrations of coordinating head groups. Potential applications of these properties include structural characterization of cation binding sites on phospholipid membranes, definition of the competition or cooperativity among different bound cations, especially in mixed lipid systems, detection and characterization of transient cation/phospholipid states, as in latteral phase changes and membrane fusion, and investigation of lattice motions, at least in the vicinity of bound cations. Although examples were given for each of these applications, the interpretations have been kept qualitative in anticipation of additional evidence.

Four of the lipids were found to exhibit more than one bound state for Tb^{3+}: DMPC, DMPE, DMPA, and cardiolipin. The two DMPC complexes have radically different structures and

are related by a lipid phase transition (Conti et al., 1987). Apparently all membrane- or micelle-forming phosphatidylcholines generate the same two complexes. The glycerol tilt, unique to membranes of this lipid class, was invoked as a constraint in forming one of the structures, but this statement raises the question of whether this feature is present in lyso-MPC micelles. With DMPE, the structure of the Tb^{3+} complex is very similar to the second DMPC complex and is invariant. The two Tb^{3+}–DMPE states appear to differ only in quantum yield. Tentatively, this may be a result of an increased exchange with the aquo species in the second state. This could arise from a more open interface due to repulsion of the cationic head group from the membrane surface (MacDonald & Seelig, 1987). Comparing DMPA, with two bound states, to DOPA, having one bound state, it was inferred that DMPA can form both tris and bis complexes with Tb^{3+}. Poorer lipid packing in DOPA apparently inhibits formation of the tris complex. Given this interpretation, as the lattice sites are occupied $Tb^{3+}\cdot(DMPA^{1-})_2$ is formed at the expense of $Tb^{3+}\cdot(DMPA^{1-})_3$. This raises some questions as to how bound cations alter the lattice structure of membranes (Copeland & Anderson, 1981a,b; Cohen & Cohen, 1981). Tb^{3+}–cardiolipin demonstrated yet a fourth type of behavior. There appears to be a single structure for the complex as signalled by an invariant 4f to 5d excitation band, but excitation through any of the 4f to 4f bands decreases in efficiency with increasing bound lanthanide. This has been interpreted as a greater sensitivity of the forbidden 4f to 4f transitions to changes in lattice vibrations (Hufner, 1978; Blasse, 1979; Jorgensen, 1979; Carnall, 1979; Reid & Richardson, 1984).

Probably the most exciting application of this probe will be in study of membrane fusion. Trivalent lanthanides have been shown to be fusogenic (Hammoudah et al., 1979; Liao & Prestegard, 1980), so it is reasonable to expect Tb^{3+} optical properties to be useful in monitoring fusion events. The mixed lipid studies, and several experiments not mentioned, have demonstrated that Tb^{3+} has an affinity for phosholipids several thousand times greater than that of Ca^{2+}. Consequently, Tb^{3+} can be introduced at low levels as a probe with displacement from the membrane only at very high relative concentrations of Ca^{2+}. In the DMPS–DMPC and cardiolipin–egg phosphatidylcholine mixed lipid studies, Tb^{3+} emission increased on a time scale of seconds to hours after addition of Ca^{2+}, with the rate depending on ionic strength, lipid ratio, and the levels of Tb^{3+} and Ca^{2+}. Before these observations can be interpreted in terms of particular membrane phase changes, it will be necessary to establish whether Tb^{3+} and Ca^{2+} coexist in the same lipid phase and the nature of the coordination change responsible for the altered Tb^{3+} emission. Given that much developmental work remains, these preliminary studies indicate that Tb^{3+} has great potential as a probe of transient cation-induced phospholipid states.

Tb^{3+} is not unique as a luminescent cation and possible Ca^{2+} mimic. Several lanthanide species are emissive (Hufner, 1978; Carnall, 1979), and two recent luminescence studies of Eu^{3+}–phospholipid complexes predate most of the studies presented here (Saris, 1983; Herrmann et al., 1986). In essence, the optical properties of Tb^{3+} and Eu^{3+} are complementary. The dramatic changes in the excitation spectrum for the various Tb^{3+}–phospholipid complexes appear to be dominated by the behavior of the 4f to 5d transitions. These gross differences will greatly facilitate the study of transient membrane states. In addition, modifications in the excitation experiments will make it possible to take advantage of a hundredfold increase in sensitivity by using the allowed 4f to 5d absorption band. Eu^{3+} lacks a low-lying 5d orbital (Hufner, 1978) and does not exhibit the dramatic spectral changes observed in these studies. Nevertheless, there are more subtle changes in the optical properties of Eu^{3+}–phospholipid complexes (Saris, 1983; Herrmann et al., 1986) which are far more amenable to a rigorous analysis of band positions and intensities in terms of structure (Hufner, 1978; Carnall, 1979; Horrocks & Sudnick, 1981; Reid & Richardson, 1984). Obviously, much remains to be attempted with these probes, which have the promise of a new perspective of cation interactions with phospholipid membranes.

ACKNOWLEDGMENTS

We thank H. Hamodi for performing the DMPA–DMPC and DOPA–DOPC mixed lipid experiments.

SUPPLEMENTARY MATERIAL AVAILABLE

Emission spectra for the 545-nm band of aquo-Tb^{3+} and complexes with DMPC, DMPE, DMPA, DMPS, DMPG, and cardiolipin (8 pages). Ordering information is given on any current masthead page.

REFERENCES

Altenbach, C., & Seelig, J. (1984) *Biochemistry 23*, 3913–3920.

Aruga, S., Kataoka, R., & Mitaku, S. (1985) *Biophys. Chem. 21*, 265–275.

Baruskov, L. I., Victorov, I. A., Evstigneera, R. P., & Bergelson, L. P. (1980) *Biochim. Biophys. Acta 598*, 153–168.

Bearer, E. L., Duzgunes, N., & Papahadjopoulos, D. (1982) *Biochim. Biophys. Acta 693*, 93–98.

Blasse, G. (1979) *Handbook on the Physics and Chemistry of Rare Earths* (Gschneidner, K. A., Jr., & Eyring, L., Eds.) Vol. 3, Chapter 24, North-Holland, Amsterdam.

Boggs, J. M., & Rangaraj, G. (1983) *Biochemistry 22*, 5425–5435.

Caffrey, M., & Feigenson, G. W. (1984) *Biochemistry 23*, 323–331.

Carnall, W. T. (1979) *Handbook on the Physics and Chemistry of Rare Earths* (Gschneidner, K. A., Jr., & Eyring, L., Eds.) Vol. 4, Chapter 34, North-Holland, Amsterdam.

Carnall, W. T., Fields, P. R., & Rajnak, K. (1968) *J. Chem. Phys. 49*, 4447–4449.

Chrzeszczyk, A., Wishnia, A., & Springer, C. S. (1981) *Biochim. Biophys. Acta 648*, 28–48.

Cohen, J. A., & Cohen, M. (1981) *Biophys. J. 36*, 623–651.

Conti, J., Halladay, H. N., & Petersheim, M. (1987) *Biochim. Biophys. Acta 902*, 53–64.

Copeland, B. R., & Andersen, H. C. (1981a) *J. Chem. Phys. 74*, 2536–2547.

Copeland, B. R., & Andersen, H. C. (1981b) *J. Chem. Phys. 74*, 2548–2558.

Dlughy, R. A., Cameron, D. G., Mantsch, H. H., & Mendelsohn, R. (1983) *Biochemistry 22*, 6318–6325.

Duzgunes, N., Paiement, J., Freeman, K. B., Lopez, N. G., Wilschut, J., & Papahadjopoulos, D. (1984) *Biochemistry 23*, 3486–3494.

Graham, I., Gagné, J., & Silvius, J. R. (1985) *Biochemistry 24*, 7123–7131.

Grasdalen, H., Eriksson, L. E. G., Westman, J., & Ehrenberg, A. (1977) *Biochim. Biophys. Acta 469*, 151–162.

Hammoudah, M. M., Nir, S., Isaac, T., Kornhauser, R., Stewart, T. P., Hui, S. W., & Vaz, W. L. C. (1979) *Biochim. Biophys. Acta 558*, 338–343.

Hauser, H., Phillips, M. C., Levine, B. A., & Williams, R. J. P. (1975) *Eur. J. Biochem. 58*, 133–144.

Herrmann, T. R., Jayaweera, A. R., & Shamoo, A. E. (1986) *Biochemistry 25*, 5834–5838.
Horrocks, W. DeW., Jr., & Sudnick, D. R. (1981) *Acc. Chem. Res. 14*, 384–392.
Horrocks, W. DeW., Jr., & Albin, M. (1984) *Prog. Inorg. Chem. 31*, 1–103.
Hufner, S. (1978) *Optical Spectra of Transparent Rare Earth Compounds*, Academic, New York.
Jorgensen, C. K. (1979) *Handbook on the Physics and Chemistry of Rare Earths* (Gschneidner, K. A., Jr., & Eyring, L., Eds.) Vol. 3, Chapter 23, North-Holland, Amsterdam.
Leventis, R., Gagné, J., Fuller, N., Rand, R. P., & Silvius, J. R. (1986) *Biochemistry 25*, 6978–6987.
Liao, M.-J., & Prestegard, J. H. (1980) *Biochim. Biophys. Acta 601*, 453–461.
MacDonald, P. M., & Seelig, J. (1987) *Biochemistry 26*, 6292–6298.
McIntosh, T. J. (1980) *Biophys. J. 29*, 237–246.
McLaughlin, A. (1982) *Biochemistry 21*, 4879–4885.
Miner, V. W., & Prestegard, J. (1984) *Biochim. Biophys. Acta 774*, 227–236.
Reid, M. F., & Richardson, F. S. (1984) *J. Phys. Chem. 88*, 3579–3586.
Saris, N.-E. L. (1983) *Chem. Phys. Lipids 34*, 1–5.
Smaal, E. B., Mandersloot, J. G., Demal, R. A., de Kruijff, B., & de Gier, J. (1987a) *Biochim. Biophys. Acta 897*, 180–190.
Smaal, E. B., Schreuder, C., van Baal, J. B., Tijberg, P. N. M., Mandersloot, J. G., de Kruijff, B., & de Gier, J. (1987b) *Biochim. Biophys. Acta 897*, 191–196.
Sundler, R., & Papahadjopoulos, D. (1981) *Biochim. Biophys. Acta 649*, 743–750.
Sundler, R., Duzgunes, N., & Papahadjopoulos, D. (1981) *Biochim. Biophys. Acta 649*, 751–758.
Verkleij, A. J. (1984) *Biochim. Biophys. Acta 779*, 43–63.
Wilschut, J., Schloma, J., Bental, M., Hoekstra, D., & Nir, S. (1985) *Biochim. Biophys. Acta 821*, 45–55.

Magnetization of the Sulfite and Nitrite Complexes of Oxidized Sulfite and Nitrite Reductases: EPR Silent Spin $S = {}^1/_2$ States†

Edmund P. Day,*,‡ Jim Peterson,‡ Jacques J. Bonvoisin,‡ Lawrence J. Young,§ James O. Wilkerson,§ and Lewis M. Siegel§

Gray Freshwater Biological Institute, University of Minnesota, P.O. Box 100, Navarre, Minnesota 55392, and Department of Biochemistry, Duke University Medical Center and Veterans Administration Hospital, Durham, North Carolina 27705

Received August 20, 1987

ABSTRACT: The saturation magnetizations of the sulfite complex of oxidized sulfite reductase and the nitrite complex of oxidized nitrite reductase have been measured to determine their spin state. Each shows the saturation magnetization signal of a spin $S = {}^1/_2$ state with $\sum g^2 = 16$, which is typical of low-spin ferrihemes. However, the EPR spectra of these complexes lack the expected signal intensity of a spin $S = {}^1/_2$ state. Indeed, one of these complexes is EPR silent. The reasons for this unexpectedly low EPR signal intensity are considered.

Sulfite reductase (SiR)[1] and nitrite reductase (NiR) are water-soluble enzymes. Each is capable of catalyzing either the six-electron reductions of sulfite to sulfide and nitrite to ammonia or the two-electron reduction of hydroxylamine to ammonia. The holoprotein of NADPH-sulfite reductase of *Escherichia coli* (EC 1.8.1.2; hydrogen sulfide:NADP$^+$ oxidoreductase) is a large (M_r 685 000) oligomeric hemoflavoprotein ($\alpha_8\beta_4$) (Siegel & Davis, 1974). The β subunit (M_r 54 600), denoted the sulfite reductase heme protein (SiR-HP), is catalytically active when reduced methylviologen (MV^+) is used as the reductant (Siegel et al., 1982). Spinach NiR (EC 1.7.7.1; ammonia:ferredoxin oxidoreductase) is very similar to SiR-HP, both in size (M_r 61 000) and in the composition of its active site (Lancaster et al., 1979).

The active site of SiR-HP consists of a siroheme (Murphy et al., 1974) antiferromagnetically exchange coupled (Christner et al., 1981) to a [4Fe-4S] cluster (Siegel, 1978). Antiferromagnetic exchange coupling is good evidence for a bridging ligand, provided the coupling is sufficiently strong ($-2J > 10$ cm^{-1}). ENDOR spectroscopy (Cline et al., 1985) argues against a nitrogenous base, such as a histidine imidazole group, as the bridging ligand between the heme and the [4Fe-4S] cluster. X-ray crystallographic studies (McRee et al., 1986) indicate that the bridge could be either a sulfur or an oxygen atom of an unidentified amino acid side chain.

Mössbauer studies of ^{57}Fe-enriched SiR-HP have established that the exchange coupling between the siroheme and the [4Fe-4S] cluster is maintained in each of three redox states and upon ligation with CN$^-$, CO, NO, or S^{2-} (Christner et al., 1983a,b, 1984). These results, and the observations that the siroheme is five-coordinate (Cline et al., 1985) and near the surface of SiR-HP with the unoccupied sixth position exposed to solvent (McRee et al., 1986), lead to the idea that exogenous

†Supported by National Institutes of Health Grants GM32394 (E.P.D.) and GM32210 (L.M.S.) and Veterans Administration Project Grant 7875-01 (L.M.S.).

‡Gray Freshwater Biological Institute.
§Duke University Medical Center and Veterans Administration Hospital.

[1] Abbreviations: EDTA, ethylenediaminetetraacetic acid; EPR, electron paramagnetic resonance; MV^+, singly reduced methylviologen dication; NADPH, nicotinamide adenine dinucleotide phosphate; NiR, spinach nitrite reductase; SiR, NADPH-sulfite reductase from *E. coli*; SiR-HP, the heme protein subunit of NADPH-sulfite reductase from *E. coli*; SQUID, superconducting quantum interference device; ENDOR, electron nuclear double resonance; DEAE, diethylaminoethyl.

0006-2960/88/0427-2126$01.50/0